Photodiagnosis and Photodynamic Therapy 28 (2019) 18–24

Contents lists available at ScienceDirect

Photodiagnosis and Photodynamic Therapy

journal homepage: www.elsevier.com/locate/pdpdt

Fluorescence photo-bleaching of urine and its applicability in oral cancer diagnosis

Surjendu Bikash Dutta[a,b], Hemant Krishna[a,c], Sharad Gupta[d], Shovan K. Majumder[a,c,*]

[a] Laser Biomedical Applications Division, Raja Ramanna Centre for Advanced Technology, Indore 452013, India
[b] Discipline of Physics, Indian Institute of Technology Indore, Indore 453552, India
[c] Homi Bhabha National Institute (HBNI), Training School Complex, Anushakti Nagar, Mumbai 400094, India
[d] Discipline of Biosciences and Biomedical Engineering, Discipline of Metallurgy Engineering and Materials Science, Indian Institute of Technology Indore, Indore 453552, India

ARTICLE INFO

Keywords:
Fluorescence spectroscopy of urine
Photo-bleaching
Classification algorithm
Double-exponential function

ABSTRACT

Photo-stability of urine is of crucial importance for the applicability of fluorescence spectroscopy of urine samples for diagnosis of cancer. We report the results of a detailed study on fluorescence photo-bleaching of human urine samples. We also present the results of a preliminary investigation on evaluation of the applicability of photo-bleaching characteristics of urine for discriminating patients with oral cancer from healthy volunteers. The time-lapse fluorescence induced by continuous shining of 405 nm radiation from a diode laser was recorded from the urine samples obtained from 18 patients with oral cancer as well as from 22 healthy volunteers with history of no known major illness in the past two months. The integrated fluorescence intensity (ΣI), calculated for each spectrum, was found to decrease with time till a point after which no further decrease was observed. Further, while significant differences were observed in the spectra of cancerous patients and healthy volunteers, these differences were found to be varying with time till the intensities of the observed fluorescence spectra corresponding to the two categories of urine samples became stable. The curve, generated by plotting ΣI vs. time, was found to be best fitted ($R^2 > 0.95$) with a double-exponential decay function. The photo-bleaching constants, obtained from curve-fitting, were found to have statistically significant differences corresponding to the urine samples of cancerous patients and healthy volunteers. A classification algorithm developed based on nearest-mean classifier (NMC) and applied on the photo-bleaching constants in leave-one-subject-out cross-validation mode was found to provide a sensitivity and specificity of up to ~ 86% in discriminating the two categories of urine samples.

1. Introduction

Urine is a natural body fluid containing rich information about the state of health of an individual. Many abnormalities in the body's metabolism get reflected both quantitatively and qualitatively in the urine constituents. Conventionally, mass spectrometry and gas chromatography are the two widely used techniques for urinalysis [1–3]. Recent reports have shown that these techniques also have the capability to detect cancer by quantitatively analyzing multiple diagnostic biomarkers (present in urine) with high sensitivity [4,5]. However, a limitation of these techniques is that these require a series of specialized sample preparation steps which are both time and chemical consuming [3]. Further, these techniques employ sophisticated and expensive instruments for urinalysis which render them unfit for the task of screening for cancer in the population at large. Thus, development of an alternate technique which is simple, reliable, inexpensive and easily accessible for mass screening is an urgent current need.

The vast body of literature on the applications of optical spectroscopy provides enough evidence to suggest that the technique has considerable prospect to be developed as a potential tool for detection of cancer based on urinalysis [6,7]. Recent research has demonstrated the potential of fluorescence spectroscopy of urine for diagnosis of various cancers including oral cancer [8–11]. Steady state fluorescence spectra were recorded from the urine samples of healthy volunteers and patients with cancer. The differences in spectral intensity distribution as well as intensities across the spectral bands of various fluorophores (believed to be present in urine) were then used for discriminating the urine samples of healthy and cancerous individuals. However, in all

* Corresponding author at: Laser Biomedical Applications Division, Raja Ramanna Centre for Advanced Technology, Indore 452013, India and Homi Bhabha National Institute (HBNI), Training School Complex, Anushakti Nagar, Mumbai 400094, India.
E-mail address: shkm@rrcat.gov.in (S.K. Majumder).

https://doi.org/10.1016/j.pdpdt.2019.08.007
Received 20 May 2019; Received in revised form 18 July 2019; Accepted 2 August 2019
Available online 05 August 2019

these studies, one common concern is that the phenomenon of photo-bleaching of urine has not been taken into account while recording its fluorescence. This is important because the onset of fluorescence photo-bleaching of urine is almost immediate (i.e. it starts as soon as one puts on the excitation light) and by the time the fluorescence measurement from a urine sample is complete, the sample is expected to have undergone considerable photo-bleaching. Now, since the temporal characteristics of photo-bleaching are not expected to be the same for all the fluorescent biomolecules comprising urine, the emission spectra measured from the same urine sample with varying integration times or at different points in time under continuous illumination could have line-shapes very different from each other. Consequently, the observed differences in the spectra of the urine samples of cancer patients and healthy individuals would completely depend on the length of time (or time delay between the start of the spectral measurement and switching of the fluorescence excitation light) one sets for recording fluorescence from each of these samples and might not remain the same even for the same set of urine samples of cancer patients and healthy individuals. As a result, the outcome of a particular discrimination model with the measured (inter-category) spectral differences [10,12–14] as its input might not be unique for a given set of urine samples belonging to cancer patients and healthy individuals. A detailed study on fluorescence photo-bleaching of human urine samples, not carried out thus far to the best of our knowledge, is therefore necessary. We report here the results of a comprehensive study on fluorescence photo-bleaching of human urine samples. We also present the results of a preliminary investigation on evaluation of the applicability of photo-bleaching characteristics of urine for discriminating patients with oral cancer from healthy volunteers.

2. Materials and methods

First morning urine samples were collected from 22 healthy volunteers who did not have any history of known major illness in the past two months, and 18 patients having cancer of oral cavity and admitted at Government cancer hospital, Indore. The volunteers were advised to maintain proper water intake in order to avoid excretion of concentrated urine. The collected urine samples were stored at 4 °C until spectroscopic measurements were performed. For acquiring spectra, the urine sample was kept in a quartz cuvette with a maximum capacity of 700 µl.

An experimental set up, developed in house, was employed for recording fluorescence spectra from the urine samples. Fig. 1 shows the experimental set up for fluorescence spectral measurement. It uses a 405 nm diode laser (of ~ 1.5 mW optical power) for sample illumination and a spectrometer for detecting the fluorescence backscattered from the sample kept in a quartz cuvette. The excitation light is focused onto the sample with a 10 X microscope objective lens. For generating a set of time-lapse fluorescence measurements from a given urine sample, spectra were acquired sequentially for 600 s at a time interval of 1 s and with an integration time of 10 ms. All the over head lamps were switched off while acquiring spectra to avoid optical noises from the surroundings. The measured spectra were corrected for system spectral response by using a NIST traceable calibration lamp (LS-1, Ocean Optics). A spectrum of white lamp was recorded and used to generate calibration factor. Each spectrum was multiplied with this calibration factor to generate the corrected spectra which were used for further analysis.

In order to identify the region of statistically spectral differences between the fluorescence spectra of urine samples from healthy volunteers and patients with oral cancer, standard error (SE) confidence intervals were utilized [15,16]. The SE was calculated at each wavelength as:

$$SE\ (\lambda) = \sqrt{\frac{\sigma^2_{Normal}(\lambda)}{n_{Normal}} + \frac{\sigma^2_{Cancer}(\lambda)}{n_{Ccancer}}}$$

Here, σ^2 is the variance of the intensities at each wavelength and n is the number of samples of a given category. The SE was then multiplied by appropriate t-values based on total degrees of freedom (DOF = $n_{Normal} + n_{Cancer} - 2$) and a predefined confidence level ($p < 0.05$) to produce a confidence interval. This helps to qualitatively identify the wavelength regions having statistically significant spectral differences. These are the wavelengths at which intensity differences between two samples types are larger than the confidence interval [15,16].

3. Results and discussions

Fig. 2a shows the typical fluorescence emission spectrum of a urine sample of a healthy volunteer measured with 405 nm excitation. The observed wavelength bands are seen to be consistent with the characteristic fluorescence emission bands reported in literature [8,9]. For example, the spectrum is characterized by a major wavelength band centered on 515 nm and a shoulder around 475 nm, and two minor wavelength bands peaking around 620 nm and 680 nm, respectively. The fluorophores responsible for the 515 nm band and the 475 nm shoulder are believed to be the co-enzymes FAD and NADH/ NADPH respectively, and that for the ~ 620 nm and ~ 680 nm bands is the porphyrin.

Fig. 2b shows the fluorescence emission spectra of the urine samples of cancer patients and healthy individuals. Each spectrum is the average of the fluorescence spectra corresponding to urine samples of the oral cancer patients and healthy volunteers and the error bars (at the peak positions) represent ± 1 standard deviation. The relative standard deviation (RSD) for the major emission band was observed to be in the range of 19–68% over the respective number of urine samples investigated. The spectra are similar to those reported in the fluorescence spectroscopic studies of urine by others [8,9,17,18]. It is apparent from the figure that the fluorescence intensities are much higher for urine samples of patients with oral cancer as compared to that for healthy volunteers. The difference spectrum obtained by subtracting the mean spectrum of urine samples of healthy volunteers from cancer patients is plotted in Fig. 2c along with 95% confidence interval at each wavelength and shown in grey band. The differences outside the grey band represent the region of statistically significant spectral differences. From the figure, it is evident that the peak around 515 nm corresponding to FAD is statistically pronounced ($p < 0.05$) in the urine spectra of cancerous patients as compared to the healthy volunteers implying a considerably larger FAD concentration in the urine of cancer patients. It is important to mention here that this is consistent with the findings reported in literature [8].

Fig. 3a and b show the emission spectra measured from the urine samples of a healthy volunteer and a patient at eight different points in time (t1 = 0 s, t2 = 50 s, t3 = 100 s, t4 = 200 s, t5 = 300 s, t6 = 400 s, t7 = 500 s and t8 = 600 s) under continuous illumination (from the 405 nm diode laser). While significant differences are observed in the spectra of cancerous patients and healthy volunteers, these differences are found to be varying with time till the intensities of the observed fluorescence spectra corresponding to the two categories of urine samples become stable. Fig. 3c shows the difference spectra derived from the set of spectra measured at different points in time from the urine samples of the same oral cancer patient and healthy volunteer. From the figure it is apparent that the inter-category spectral differences are varying significantly till t = 200 s beyond which it is found to remain almost constant.

In order to see whether this observed variation in the inter-category spectral differences has any effect on the efficacy in separating the urine samples of cancerous patients from those of healthy volunteers, spectrally integrated intensities (ΣI) were estimated from the full set of

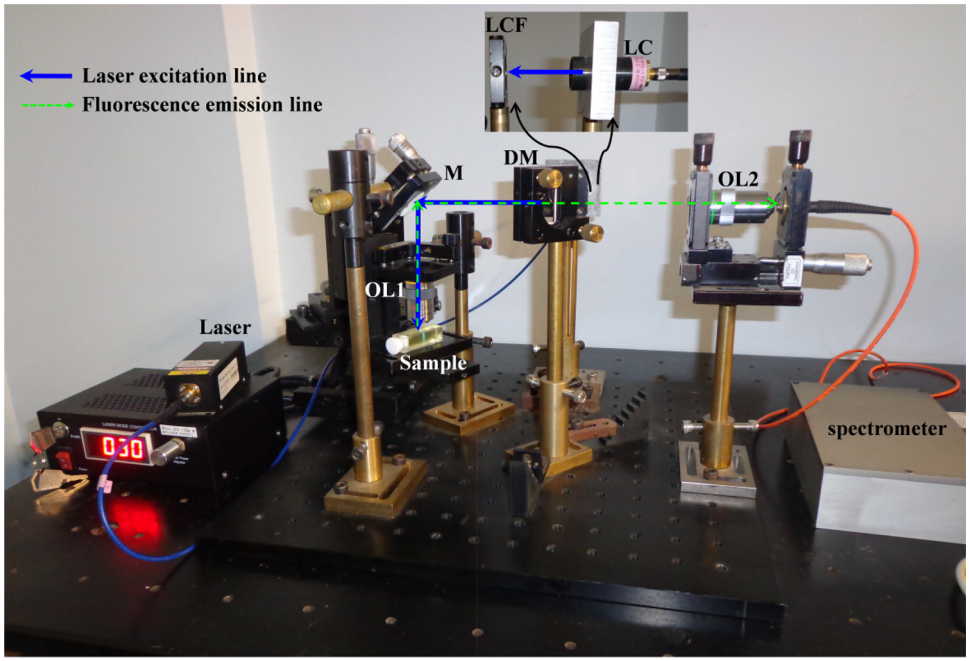

Fig. 1. Experimental set-up for measurements of fluorescence spectra of urine samples. The abbreviations and their corresponding expansions are as follow: LC – Laser collimator, LCF – Laser clean-up filter, DM – Dichroic mirror, M – Mirror, OL1 – Objective lens 1, OL2 – Objective lens 2.

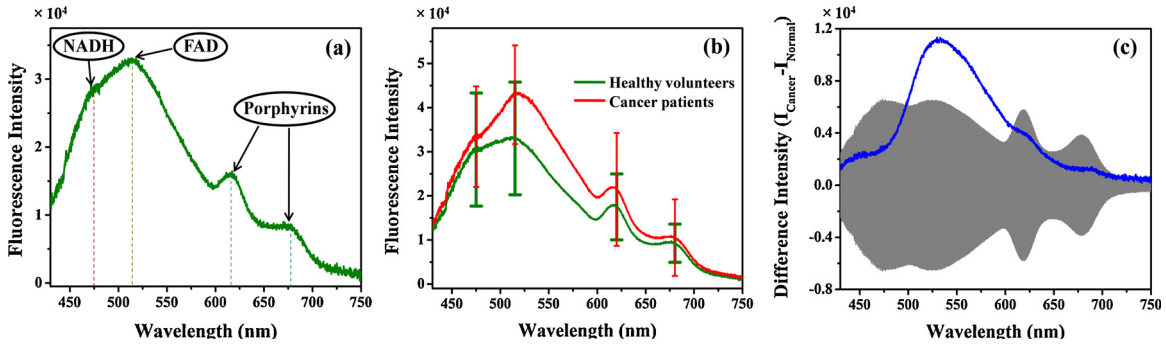

Fig. 2. (a) Fluorescence spectrum of the urine sample of a healthy volunteer. The healthy volunteer was chosen randomly out of 22 healthy volunteers. **(b)** Mean fluorescence spectra of urine samples corresponding to patients with oral cancer and healthy volunteers. Each spectrum is the average of the spectra over urine samples of 22 healthy volunteers and 18 oral cancer patients. **(c)** Mean difference spectra showing statistical differences between fluorescence spectra of cancer patients and healthy volunteers. Grey bands indicate 95% confidence intervals of the difference determined by standard error confidence intervals. The spectrum from each of the patients and healthy volunteers was measured immediately following putting on of the illumination laser.

fluorescence spectra of urine samples of patients and healthy subjects acquired at different time-points of measurements, and used as input to a classification algorithm developed based on nearest mean classifier (NMC) [19,20]. A nearest mean-classifier is based on the least Euclidean distance of the test data from the means of the prototype data of the corresponding classes in the training set [19–21]. The algorithm was applied on the ΣI values in leave-one-subject-out-cross validation mode. In this method, training of the algorithm is performed using data

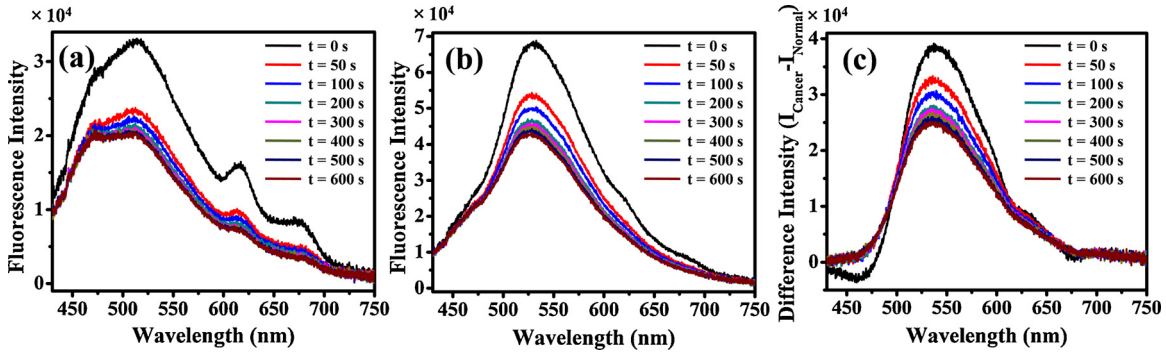

Fig. 3. Fluorescence spectra measured from the urine samples of **(a)** a healthy volunteer, **(b)** a patient at eight different points in time following putting on of the illumination light. **(c)** The difference spectra between the urine samples of the same patient and the healthy volunteer corresponding to those time points.

Table 1
The classification results yielded by the nearest mean classifier based classification algorithm in discriminating urine samples of the oral cancer patients (n = 18) from that of the healthy volunteers (n = 22) using spectrally integrated intensities estimated from the fluorescence spectra measured at different points in time following putting on of the illumination light as input. The classification results are based on leave-one-subject-out cross validation.

Acquisition time (s)	Sensitivity	Specificity	Overall accuracy
At t = 0	72%	73%	72%
At t = 50	67%	73%	70%
At t = 100	61%	73%	68%
At t = 200	61%	68%	65%
At t = 300	61%	68%	65%
At t = 400	61%	68%	65%
At t = 500	61%	68%	65%
At t = 600	61%	68%	65%

of urine samples of N-1 subjects (N being the total number of subjects) and test is carried out only on the data of the urine sample of the excluded subject. Table 1 lists the sensitivities and specificities yielded by the NMC based classification algorithm. One can see that the sensitivity and specificity values are decreasing with time and are also different for the different sets of spectra acquired till t = 200 s. Since the primary basis of discrimination between the urine samples is the observed differences in the urine spectra of patients and healthy volunteers, the varying spectral differences resulted at different time points of measurements (under continuous illumination) have led to varying results of discrimination even for the same set of urine samples of cancer patients and healthy subjects. However, the sensitivity and specificity values are found to remain the same for the remaining sets of spectra acquired at t > 200 s since no appreciable variation in the spectral differences is observed for these sets of spectra measured at t > 200 s.

In order to understand the temporal characteristics of reduction in the intensities of the urine fluorescence, ΣI values estimated from the fluorescence spectra (shown in Fig. 3) of urine samples of the healthy volunteer and the oral cancer patient were plotted against the different time-points of spectral measurements. Fig. 4 shows the plot of ΣI as a function of time-points of measurements. It is apparent from the figure that the urine sample from the healthy subject has faster rate of fluorescence photo-bleaching as compared to the urine sample of the patient with oral cancer. For quantifying this inter-category difference in the temporal characteristics of the reduction in fluorescence (i.e. fluorescence photo-bleaching), the ΣI verses time-point of spectral

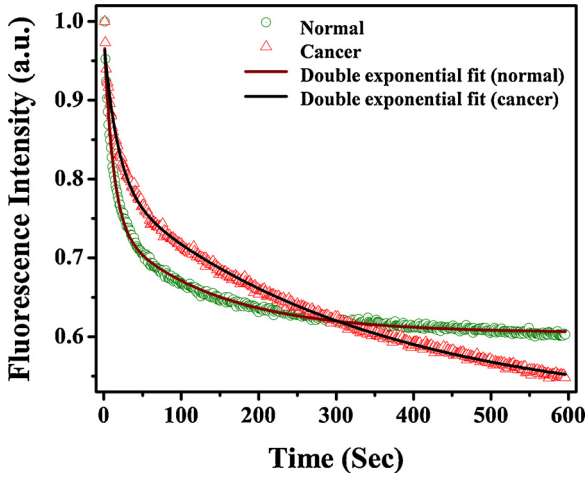

Fig. 4. Plot of integrated fluorescence intensities as a function of time-points of measurements for the urine samples belonging to a healthy volunteer and a cancer patient. The solid line represents the double-exponential fit to the measured data.

Table 2
The fast (τ_1) and slow (τ_2) photo-bleaching time constants corresponding to the urine samples of cancer patients and healthy individuals.

Health state	τ_1 (s)	τ_2 (s)
Normal	7.6 ± 3.6	107.9 ± 44.3
Cancer	16.0 ± 3.8	216.7 ± 67.5

measurements curves were fitted with a double-exponential decay function given by:

$$\Sigma I(t) = A + B\exp^{-t/\tau_1} + C\exp^{-t/\tau_2}$$

where A, B and C are constants, τ_1 and τ_2 are the time constants for the fast and slow phases of photo-bleaching, t is the time and ΣI (t) is the spectrally integrated intensity as a function of time. Fig. 4 shows the double-exponential fits to the ΣI verses time-point of spectral measurements curves for the urine samples of the healthy subject and the oral cancer patient. The fits were found to result in a R^2 value of ~0.99. The double exponential behavior can be attributed to the Gaussian profile of the excitation laser beam which leads to inhomogeneous power distribution along the transverse plane [22]. The constant of the faster photo-bleaching represents the molecules exposed by the high intensity region near the axis, whereas the slower photo-bleaching constant is due to the outermost low intensity region of the laser [22,23].

Table 2 shows the mean ± standard deviation (σ) of the photo-bleaching time-constants, τ_1 and τ_2, estimated from the ΣI verses time-point of spectral measurements curves of the urine samples belonging to all the healthy subjects and the patients with oral cancer. It can be seen that both the fast (τ_1) and slow (τ_2) time-constants are considerably smaller in urine samples obtained from the healthy volunteers as compared to that from patients with oral cancer. A Student's t-test confirmed that the differences in the mean values of these time constants between the two categories (cancer and normal) were indeed statistically significant ($p < 0.001$). Fig. 5 shows a graphical presentation of the fast (τ_1) versus slow (τ_2) time constants for the urine samples corresponding to patients with oral cancer and healthy subjects. The graph is plotted along with a probability ellipsoid around each of the urine sample categories. The probability ellipsoid [24] around a category (of data) defines the region that contains 90% of data belonging to that category assuming Gaussian distribution. Thus from the probability ellipsoids shown in Fig. 5 it is apparent that there is significant separation between the urine samples belonging to patients with oral cancer and healthy subjects. In order to further quantify the

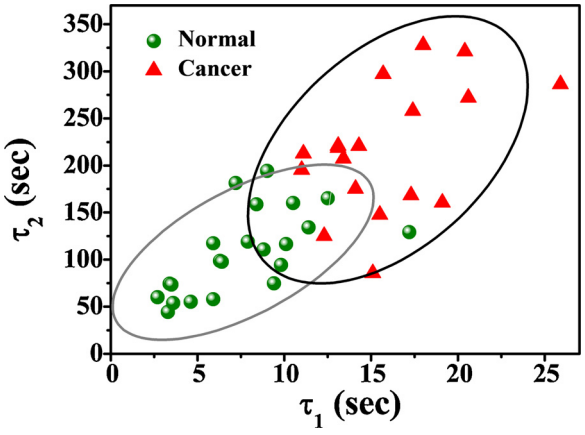

Fig. 5. A graphical presentation of the fast (τ_1) versus slow (τ_2) photo-bleaching time constants for the urine samples corresponding to patients with oral cancer and healthy subjects. The graph is plotted along with a 90% probability ellipsoid around each of the urine sample categories.

Table 3
The classification results yielded by the nearest mean classifier based classification algorithm in discriminating urine samples of the oral cancer patients from that of the healthy volunteers using fast (τ_1) and slow (τ_2) photo-bleaching time constants estimated from the curve-fitting analyses. The classification results are based on leave-one-subject-out cross validation.

Pathology diagnosis	Sensitivity	Specificity	Overall accuracy
Normal (n = 22) vs. Cancer (n = 18)	78%	86%	82%

potential of the photo-bleaching time-constants in discriminating the two categories of urine samples, the NMC based algorithm [19–21] was employed in leave-one-sample-out cross validation mode where the values of the time constants were used as input. Table 3 lists the sensitivity and specificity values yielded by the algorithm in discriminating the urine samples belonging to patients with oral cancer and healthy subjects. The sensitivity and specificity were found to be 78% and 86%, respectively. One can see that by considering the temporal characteristics of photo-bleaching of urine samples, the overall classification accuracy was improved to 82% as compared to the maximum of 72% obtained when the integrated fluorescence intensity was considered for classification (Table 1).

After establishing the applicability of the photo-bleaching time constants in discriminating urine samples of the oral cancer patients from that of the healthy subjects, the next important task was to find out the underlying reason for the differences in the temporal patterns of photo-bleaching for the two categories of urine samples. In order for that fluorescence emission spectra measured from all the urine samples belonging to the two categories (i.e. patients with oral cancer and healthy subjects) at different points in time under continuous illumination were spectrally decomposed into a set of three basis spectra corresponding to the emission spectra of NADH, FAD, and porphyrins respectively. The choice of these basis set spectra was guided by the fact that the human urine samples are known to contain three major fluorophores, NADH, FAD and Protoporphyrin IX that could be excited by light of 405 nm wavelength [8,9,25]. The first step towards carrying out the spectral decomposition is generation of the basis set spectra. For that, the fluorescence emission spectra of the authentic NADH, FAD and Protoporphyrin IX were recorded using 405 nm excitation in the same experimental set up used to measure the spectra of urine samples. The spectra were then peak-normalized and linearly combined to fit the measured time-lapse fluorescence emission of the different urine samples belonging to the two different categories. The linear fit is justified in this case because urine, having very little or almost no turbidity, can be considered as a solution very close to a dilute solution. Fig. 6 shows the peak-normalized fluorescence emission spectra of NADH, FAD and porphyrins. It is apparent from the figure that while the fluorescence spectra of NADH and FAD are characterized by single emission bands, the porphyrin fluorescence spectrum shows two emission bands. The results of the spectral fitting analyses are graphically demonstrated in Fig. 7. The spectral fitting is shown for a set of two urine samples, one corresponding to a healthy subject and the other corresponding to a patient with oral cancer. One can clearly see that the relative contribution of the spectral band, characteristics of FAD, is more in urine samples of the cancer patients than that of the healthy subject. It is pertinent to note that a similar increase was obtained by Al-Salhi et al. [26] for the urine samples of cancer patients with 400 nm excitation and attributed to an increase in FAD concentration [27]. However, it is apparent from the figure that there is no significant difference in the relative contribution of NADH or porphyrins between the two categories of urine samples. This is supported by the difference spectrum shown in Fig. 2c where it is observed that their absolute contributions in the spectra of urine samples of the cancer patient and the healthy subject are within the limit of inter-subject variation.

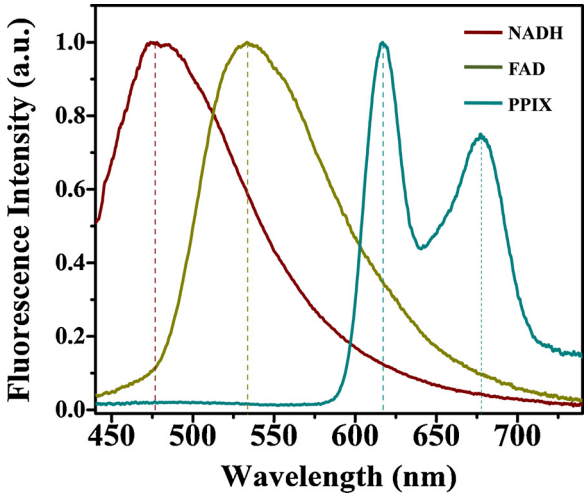

Fig. 6. The peak normalized fluorescence emission spectra of reduced Nicotinamide Adenine Dinucleotide (NADH), Flavin Adenine Dinucleotide (FAD) and Protoporphyrin IX (PPIX).

Table 4 lists the fast (τ_1) and slow (τ_2) photo-bleaching time constants corresponding to NADH, FAD and porphyrins, respectively, obtained from the spectral fitting of the measured time-lapse fluorescence emission spectra of the full set of urine samples belonging to patients with oral cancer and healthy subjects. A perusal of the table shows: (i) both τ_1 and τ_2 corresponding to NADH are significantly smaller ($p < 0.05$) as compared to FAD in the urine samples of both the cancer patients and healthy subjects implying faster photo-bleaching rate of NADH in comparison with FAD (ii) τ_2 of FAD is much larger for the urine of the cancer patients than the urine of the healthy subjects suggesting slower photo-bleaching of urine in the cancer patients, and (iii) no statistically significant differences in τ_1 and τ_2 corresponding to NADH and porphyrins are observed between the urine samples of the cancer patients and that of the healthy subjects suggesting that these fluorophores seem to have no or little contribution in the observed differences in the temporal patterns of photo-bleaching of urine belonging to the two categories. These observations are in qualitative agreement with the photo-bleaching time constants of the urine samples of the cancer patients and healthy subjects tabulated in Table 2. In particular it is important to note here that the observed photo-bleaching time-constants of the urine of the cancer patients are found to be close in value to the time-constants estimated for FAD. This is plausibly due to the fact that the urine of cancer patients is reported to contain significantly larger FAD [8,9,26,27]. The photo-bleaching rates also depend upon the chemical environment in which the fluorophores are present [28–30]. This might also be the reason for variations in the time constants of the same fluorophore in urine of cancer patients and healthy subjects.

The primary objective of the present study was to understand the fluorescence photo-bleaching characteristics of human urine samples and show how the use of urine fluorescence which was still undergoing photo-bleaching could lead to discrimination results very different from what was obtained when it was used after becoming stable following the completion of photo-bleaching. The other important objective was to assess the discrimination ability of the photo-bleaching time constants in separating the urine samples of cancer patients and healthy individuals. For performing both these tasks, a supervised classifier which is simple enough in its mathematical formulation and does not require optimization of any of its design parameters, while being trained, was sufficient. NMC being a geometric classifier and its performance solely being dependent on the linear separation of spectral data at disposal, unlike a statistical classifier whose performance also depends on the optimization of algorithm parameters for each of the

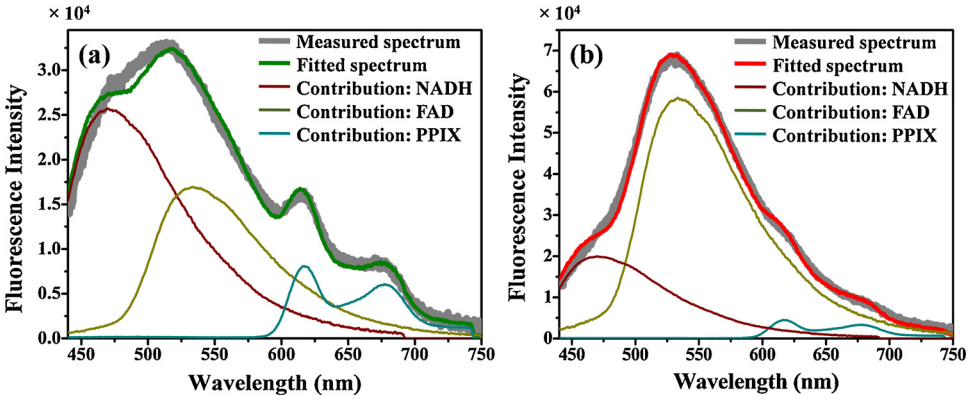

Fig. 7. Fluorescence spectra measured immediately following putting on of the illumination laser from urine samples corresponding to **(a)** a healthy volunteer and **(b)** a patient with oral cancer. Each spectrum was fitted with peak-normalized emission spectra of NADH (solid blue line), FAD (solid purple line) and Protoporphyrin IX (solid magenta line).

Table 4
The fast (τ_1) and slow (τ_2) photo-bleaching time constants corresponding to NADH, FAD and porphyrins, respectively, obtained from the spectral fitting of the measured time-lapse fluorescence emission spectra of the full set of urine samples belonging to patients with oral cancer and healthy subjects.

Fluorophores	Health state	τ_1 (s)	τ_2 (s)
NADH	Normal	5.6 ± 3.7	84.7 ± 63.9
	Cancer	6.3 ± 3.2	109.2 ± 90.1
FAD	Normal	12.5 ± 3.5	167.5 ± 31.6
	Cancer	19.5 ± 2.7	231.7 ± 52.3
PPIX	Normal	13.3 ± 3.7	145.45 ± 17.4
	Cancer	12.2 ± 5.1	155.6 ± 59.4

classification tasks, was therefore deemed appropriate for the present job.

However, it should be noted here that in the next phase of our study (already in progress) where the objective is to establish a model of oral cancer diagnosis based on fluorescence photo-bleaching data of large population of patients, we will be employing a probability based statistical classification algorithm [31], which was developed earlier based on the mathematical formulation of sparse multinomial logistic regression [32] and used in several of our earlier studies [33–35]. The algorithm was found to provide best classification accuracy of 92% (leave-one-out cross validation mode) as compared to that of 82% using NMC. However, when the algorithm was applied in "no cross validation mode" (i.e. same set of data used for both training and validation), the classification accuracy was 100%.

4. Conclusions

To conclude, a detailed study on fluorescence photo-bleaching of human urine samples was carried out. The time lapse fluorescence spectra were recorded from the urine samples obtained from patients with oral cancer as well as from healthy volunteers under continuous illumination of 405 nm radiation from a diode laser. It was found that while significant differences existed in the spectra of cancerous patients and healthy volunteers, these differences were varying with time till the intensities of the observed fluorescence spectra corresponding to the two categories of urine samples became stable. In order to quantify the spectral differences, integrated fluorescence intensity (ΣI) was calculated for each spectrum and a classification algorithm developed based on NMC was applied in leave-one-subject-out cross-validation mode on ΣI values for each of the sets of spectra measured from the two categories of the urine samples at different points in time. The sensitivity and specificity values yielded by the algorithm were found to decrease till t = 200 s beyond which they were found to remain almost unchanged. A decay curve was generated by plotting ΣI vs. time and fitted with a double-exponential decay function. The photo-bleaching constants, obtained from curve-fitting, were found to have statistically significant differences corresponding to the urine samples of cancerous patients and healthy volunteers. The NMC based classification algorithm applied on the photo-bleaching constants in leave-one-subject-out cross-validation mode was found to provide a sensitivity and specificity of up to 86% in discriminating the two categories of urine samples. Overall, the results of the studies showed that the temporal characteristic of photo-bleaching had promising potential to be used as an alternate tool for oral cancer diagnosis.

Acknowledgement

One of the authors, Mr. Surjendu Bikash Dutta, would also like to acknowledge Indian Institute of Technology, Indore for providing financial assistance in carrying out his research.

References

[1] M.M. Khamis, D.J. Adamko, A. El-Aneed, Mass spectrometric based approaches in urine metabolomics and biomarker discovery, Mass Spectrom. Rev. 36 (2) (2017) 115, https://doi.org/10.1002/mas.21455.
[2] Y.-T. Chen, C.-H. Tsai, C.-L. Chen, J.-S. Yu, Y.-H. Chang, Development of biomarkers of genitourinary cancer using mass spectrometry-based clinical proteomics, J. Food Drug Anal. 27 (2) (2019) 387, https://doi.org/10.1016/j.jfda.2018.09.005.
[3] K.K. Pasikanti, P.C. Ho, E.C.Y. Chan, Gas chromatography/mass spectrometry in metabolic profiling of biological fluids, J. Chromatogr. B 871 (2) (2008) 202, https://doi.org/10.1016/j.jchromb.2008.04.033.
[4] R.B.M. Aggio, B. de Lacy Costello, P. White, T. Khalid, N.M. Ratcliffe, R. Persad, C.S.J. Probert, The use of a gas chromatography-sensor system combined with advanced statistical methods, towards the diagnosis of urological malignancies, J. Breath Res. 10 (1) (2016) 17106, https://doi.org/10.1088/1752-7155/10/1/017106.
[5] M. Cauchi, C.M. Weber, B.J. Bolt, P.B. Spratt, C. Bessant, D.C. Turner, C.M. Willis, L.E. Britton, C. Turner, G. Morgan, Evaluation of gas chromatography mass spectrometry and pattern recognition for the identification of bladder cancer from urine headspace, Anal. Methods 8 (20) (2016) 4037, https://doi.org/10.1039/C6AY00400H.
[6] R.A. Shaw, S. Kotowich, H.H. Mantsch, M. Leroux, Quantitation of protein, creatinine, and urea in urine by near-infrared spectroscopy, Clin. Biochem. 29 (1) (1996) 11, https://doi.org/10.1016/0009-9120(95)02011-X.
[7] J. Kušnír, K. Dubayova, L. Lešková, M. Lajtar, Concentration matrices—solutions for fluorescence definition of urine, Anal. Lett. 38 (10) (2005) 1559, https://doi.org/10.1081/AL-200065787.
[8] V. Masilamani, V. Trinka, M. Al Salhi, K. Govindaraj, A.P. Raghavan, B. Antonisamy, Cancer detection by native fluorescence of urine, J. Biomed. Opt. 15 (5) (2010) 57003, https://doi.org/10.1117/1.3486553.
[9] V. Masilamani, M.S. AlSalhi, T. Vijmasi, K. Govindarajan, R.R. Rai, M. Atif, S. Prasad, A. Aldwayyan, Fluorescence spectra of blood and urine for cervical cancer detection, J. Biomed. Opt. 17 (9) (2012) 98001, https://doi.org/10.1117/1.JBO.17.9.098001.
[10] R. Pachaiappan, A. Prakasarao, A. Kesavan, G. Singaravelu, Native fluorescence spectroscopy: an optical tool in delineating oral cancer patients from normal subjects and diabetic patients using urine, 2017 Trends in Industrial Measurement and Automation (TIMA) IEEE 6 (2017) 1–4, https://doi.org/10.1109/TIMA.2017.8064822.
[11] R. Rajasekaran, P.R. Aruna, D. Koteeswaran, L. Padmanabhan, K. Muthuvelu, R.R. Rai, P. Thamilkumar, C. Murali Krishna, S. Ganesan, Characterization and diagnosis of cancer by native fluorescence spectroscopy of human urine, Photochem. Photobiol. 89 (2) (2013) 483–491, https://doi.org/10.1111/j.1751-1097.2012.01239.x.
[12] M. Zvarik, D. Martinicky, L. Hunakova, I. Lajdova, L. Sikurova, Fluorescence

characteristics of human urine from normal individuals and ovarian cancer patients, Neoplasma 60 (5) (2013) 533–537, https://doi.org/10.4149/neo_2013_069.
[13] M. Atif, M.S. AlSalhi, S. Devanesan, V. Masilamani, K. Farhat, D. Rabah, A study for the detection of kidney cancer using fluorescence emission spectra and synchronous fluorescence excitation spectra of blood and urine, Photodiagn. Photodyn. Ther. 23 (2018) 40–44, https://doi.org/10.1016/j.pdpdt.2018.05.012.
[14] R. Rajasekaran, P.R. Aruna, D. Koteeswaran, G. Bharanidharan, M. Baludavid, S. Ganesan, Steady-state and time-resolved fluorescence spectroscopic characterization of urine of healthy subjects and cervical cancer patients, J. Biomed. Opt. 19 (3) (2014) 37003, https://doi.org/10.1117/1.JBO.19.3.037003.
[15] C.A. Lieber, S.K. Majumder, D.L. Ellis, D.D. Billheimer, A. Mahadevan-Jansen, In vivo nonmelanoma skin cancer diagnosis using Raman microspectroscopy, Lasers Surg. Med. 40 (7) (2008) 461–467, https://doi.org/10.1002/lsm.20653.
[16] H. Krishna, S. Muttagi, P. Ingole, P. Chaturvedi, S.K. Majumder, Tobacco consumption induced changes in the healthy oral mucosa and its effect on differential diagnosis of oral lesions—a clinical in vivo raman spectroscopic study, J. Anal. Oncol. 5 (3) (2016) 110–123, https://doi.org/10.6000/1927-7229.2016.05.03.4.
[17] M. AlSalhi, A.A. Mehmadi, A.A. Abdo, S. Prasad, V. Masilamani, Diagnosis of liver cancer and cirrhosis by the fluorescence spectra of blood and urine, Technol. Cancer Res. Treat. 11 (4) (2012) 345–351, https://doi.org/10.7785/tcrt.2012.500282.
[18] M.S. AlSalhi, A.M. Al Mehmadi, A. Abdoo, V. Masilamani, Liver cancer diagnosis by fluorescence spectra of blood and urine, Tenth International Conference on Photonics and Imaging in Biology and Medicine (PIBM 2011) 8329 (2012) 83290X, https://doi.org/10.1117/12.923788.
[19] P. Datta, D. Kibler, Symbolic nearest mean classifiers, AAI/IAAI (1997) 82–87 https://www.aaai.org/Papers/AAAI/1997/AAAI97-013.pdf.
[20] S.K. Majumder, N. Ghosh, P.K. Gupta, Relevance vector machine for optical diagnosis of cancer, Lasers Surg. Med. 36 (4) (2005) 323–333, https://doi.org/10.1002/lsm.20160.
[21] S.K. Majumder, N. Ghosh, P.K. Gupta, Support vector machine for optical diagnosis of cancer, J. Biomed. Opt. 10 (2) (2005) 24034, https://doi.org/10.1117/1.1897396.
[22] A.J. Berglund, Nonexponential statistics of fluorescence photobleaching, J. Chem. Phys. 121 (7) (2004) 2899–2903, https://doi.org/10.1063/1.1773162.
[23] S. Gupta, P. Goswami, A. Agarwal, A. Pradhan, Experimental and theoretical investigation of fluorescence photobleaching and recovery in human breast tissue and tissue phantoms, Appl. Opt. 43 (5) (2004) 1044–1052, https://doi.org/10.1364/AO.43.001044.
[24] L.C. Adkins, R. Carter Hill, An improved confidence ellipsoid for the linear regression model, J. Stat. Comput. Simul. 36 (1) (1990) 9–18, https://doi.org/10.1080/00949659008811249.
[25] M. Inaguma, K. Hashimoto, Porphyrin-like fluorescence in oral cancer: in vivo fluorescence spectral characterization of lesions by use of a near-ultraviolet excited autofluorescence diagnosis system and separation of fluorescent extracts by capillary electrophoresis, Cancer 86 (11) (1999) 2201–2211, https://doi.org/10.1002/(SICI)1097-0142(19991201)86:11<2201::AID-CNCR5>3.0.CO;2-9.
[26] M. Al-Salhi, V. Masilamani, T. Vijmasi, H. Al-Nachawati, A.P. VijayaRaghavan, Lung cancer detection by native fluorescence spectra of body fluids—a preliminary study, J. Fluoresc. 21 (2) (2011) 637–645, https://doi.org/10.1007/s10895-010-0751-9.
[27] R. Rajasekaran, P. Aruna, D. Koteeswaran, M. Baludavid, S. Ganesan, Synchronous luminescence spectroscopic characterization of urine of normal subjects and cancer patients, J. Fluoresc. 24 (4) (2014) 1199–1205, https://doi.org/10.1007/s10895-014-1401-4.
[28] L. Song, E.J. Hennink, I.T. Young, H.J. Tanke, Photobleaching kinetics of fluorescein in quantitative fluorescence microscopy, Biophys. J. 68 (6) (1995) 2588–2600, https://doi.org/10.1016/S0006-3495(95)80442-X.
[29] D.M. Benson, J. Bryan, A.L. Plant, A.M. Gotto, L.C. Smith, Digital imaging fluorescence microscopy: spatial heterogeneity of photobleaching rate constants in individual cells, J. Cell Biol. 100 (4) (1985) 1309–1323, https://doi.org/10.1083/jcb.100.4.1309.
[30] D. Wüstner, T. Christensen, L. Solanko, D. Sage, Photobleaching kinetics and time-integrated emission of fluorescent probes in cellular membranes, Molecules 19 (8) (2014) 11096–11130, https://doi.org/10.3390/molecules190811096.
[31] S.K. Majumder, S. Gebhart, M.D. Johnson, R. Thompson, W.C. Lin, A. Mahadevan-Jansen, A probability-based spectroscopic diagnostic algorithm for simultaneous discrimination of brain tumor and tumor margins from normal brain tissue, Appl. Spectrosc. 61 (5) (2007) 548–557, https://doi.org/10.1366/000370207780807704.
[32] B. Krishnapuram, L. Carin, M.A. Figueiredo, A.J. Hartemink, Sparse multinomial logistic regression: fast algorithms and generalization bounds, IEEE Trans. Pattern Anal. Mach. Intell. 27 (6) (2005) 957–968, https://doi.org/10.1109/TPAMI.2005.127.
[33] S.K. Majumder, M.D. Keller, F.I. Boulos, M.C. Kelley, A. Mahadevan-Jansen, Comparison of autofluorescence, diffuse reflectance, and Raman spectroscopy for breast tissue discrimination, J. Biomed. Opt. 13 (5) (2008) 54009, https://doi.org/10.1117/1.2975962.
[34] H. Krishna, S.K. Majumder, P. Chaturvedi, M. Sidramesh, P.K. Gupta, In vivo Raman spectroscopy for detection of oral neoplasia: a pilot clinical study, J. Biophotonics 7 (9) (2014) 690–702, https://doi.org/10.1002/jbio.201300030.
[35] H. Krishna, S.K. Majumder, P. Chaturvedi, P.K. Gupta, Anatomical variability of in vivo Raman spectra of normal oral cavity and its effect on oral tissue classification, Biomed. Spectrosc. Imaging 2 (3) (2013) 199–217, https://doi.org/10.3233/BSI-130042.